

## Field-Aligned Plasma-Potential Structure Formed by Local Electron Cyclotron Resonance

HATAKEYAMA Rikizo\*, KANEKO Toshiro and SATO Noriyoshi  
Graduate School of Engineering, Tohoku University, Sendai 980-8579, Japan

(Received: 5 December 2000 / Accepted: 27 August 2001)

### Abstract

The significance of basic experiments on field-aligned plasma-potential structure formed by local electron cyclotron resonance (ECR) is claimed based on the historical development of the investigation on electric double layer and electrostatic potential confinement of open-ended fusion-oriented plasmas. In the presence of a single ECR point in simple mirror-type configurations of magnetic field, a potential dip (thermal barrier) appears around this point, being followed by a subsequent potential hump (plug potential) along a collisionless plasma flow. The observed phenomenon gives a clear-cut physics to the formation of field-aligned plug potential with thermal barrier, which is closely related to the double layer formation triggered by a negative dip.

### Keywords:

field-aligned structure, local electron cyclotron resonance, plug/barrier potential, effective confinement

### 1. Introduction

The formation and control of plasma potential along magnetic-field lines has attracted general attention in laboratory, space and fusion-oriented plasmas because the potential structure holds the key of wave-nonlinear development, charged-particle acceleration, plasma confinement and heat-transport reduction. In that connection, local electron cyclotron resonance (ECR) as a typical principle of radio-frequency heating in inhomogeneous magnetic fields is endowed with important attribute, because it is supposed to induce interruption of field-aligned electron flow, resulting in the formation of local plasma-potential structure under the charge neutrality condition. This process can be applied to heat-flux control in diverted torus plasmas, where the combination of  $\nabla B$  along a divertor channel and ECR heating (ECRH) could yield thermal dike formation [1]. It can also be applied to improved confinement in tandem-mirror plasmas. Historically speaking, the original tandem-mirror scenario for plug/

barrier potential formation [2] simultaneously required a neutral beam injection (NBI) producing sloshing ions and two ECR points in each cell. This scenario was demonstrated by the TMX-U [3] and GAMMA 10 [4] experiments in 1984 and 1985, respectively.

In this stage, however, we pointed out that the underlying physics of the above-mentioned idea is related to double-layer formation [5] triggered by a small potential dip inducing current limitation. Actually in a laboratory experiment in 1980, we could already find the potential dip and rise like the plug/barrier in a DC-discharge positive column [6]. The same was found in a particle simulation in 1980 [7]. Therefore, we claimed that only a single ECR point is sufficient for the plug/barrier formation. Thereafter, our basic experiments have demonstrated this novel scenario [8]. On the other hand, recent GAMMA 10 experiments have shown in 1995 that the plug/barrier potential is formed without NBI in the presence of the two ECR

\*Corresponding author's e-mail: [hatake@ecei.tohoku.ac.jp](mailto:hatake@ecei.tohoku.ac.jp)

points in each cell [9]. Furthermore, only fundamental ECRH, i.e., the single ECRH is now used to produce the plug/barrier potential in the GAMMA 10 experiments [10].

Thus, in order to systematically clarify essential features of the problem, it has been required to investigate details of potential formation and control due to local ECR under simplified configurations. Here, three kinds of basic experiments are carried out using a single-ended Q machine. Secondly, a comparison between our results and GAMMA 10 results is made. Thirdly, a particle-in-cell (PIC) computer simulation is performed.

## 2. Experimental Apparatus

A collisionless plasma is produced by surface ionization of potassium atoms on a hot tungsten plate under an electron-rich condition and is confined by a magnetic field  $B$  of a few kG in the  $Q_T$ -Upgrade machine, as shown schematically in the upper figure in Fig. 1. A plasma-flow pulse is injected along the magnetic field ( $t = 0$ ) by applying a step potential  $\phi_g$  to a negatively-biased grid in front of the hot plate. A small Langmuir probe is used to measure plasma parameters and their axial profile. The plasma density, electron and ion temperatures, and ion flow energy are  $n_0 \approx 1 \times 10^9 \text{ cm}^{-3}$ ,  $T_{e0} \approx 0.2 \text{ eV}$ ,  $T_{i0} \lesssim T_{e0}$ , and  $E_{i0} \approx 10T_{e0}$ , respectively. A background gas pressure is  $4 \times 10^{-7} \text{ Torr}$ .

A microwave with frequency  $\omega/2\pi = 6 \text{ GHz}$  and power  $P_\mu = 0 - 1 \text{ W}$  is launched into the plasma through

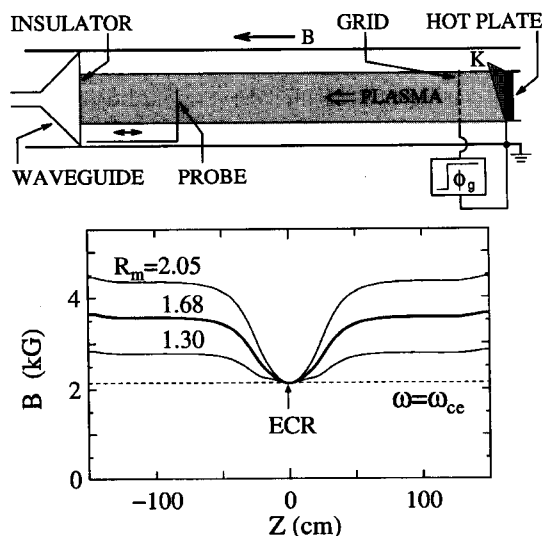


Fig. 1 Schematic of experimental setup and symmetric magnetic-well configuration.

a circular waveguide at the other end of the machine ( $z = -150 \text{ cm}$ ), propagating toward the hot plate ( $z = 160 \text{ cm}$ ). The subscript 0 stands for the parameters in the case of  $P_\mu = 0 \text{ W}$ .

## 3. Experimental Results and Discussion

The first experiment is concerned with a single-point resonance in symmetric magnetic-well configurations as shown in the lower figure in Fig. 1. The bottom of the magnetic well is located at the machine center. A mirror ratio  $R_m$  is defined as the ratio of  $B$  around  $z = \pm 100 \text{ cm}$  to that at  $z = 0 \text{ cm}$ . The profile for  $R_m = 1.68$  is typically used in the following experiment. The microwave propagates toward the right-hand side in the region of  $\omega/\omega_{ce} < 1$  and the ECR takes place in the vicinity of  $\omega/\omega_{ce} = 1$  ( $\omega_{ce}/2\pi$ : electron cyclotron frequency) denoted by the arrow at  $z = 0 \text{ cm}$ .

Figure 2 shows typical profiles of plasma potential  $\phi$  and electron density  $n_e$  in the case of  $R_m = 1.68$  and  $P_\mu = 0.5 \text{ W}$  at  $t = 0.6 \text{ msec}$  which corresponds to the time necessary for the plasma flow to arrive at the ECR region. The potential structure consists of a potential dip  $\Delta\phi_d (< 0)$  formed around the ECR point and a subsequent potential hump  $\Delta\phi_p (> 0)$  along the plasma flow.  $n_e$  gradually decreases toward the downstream

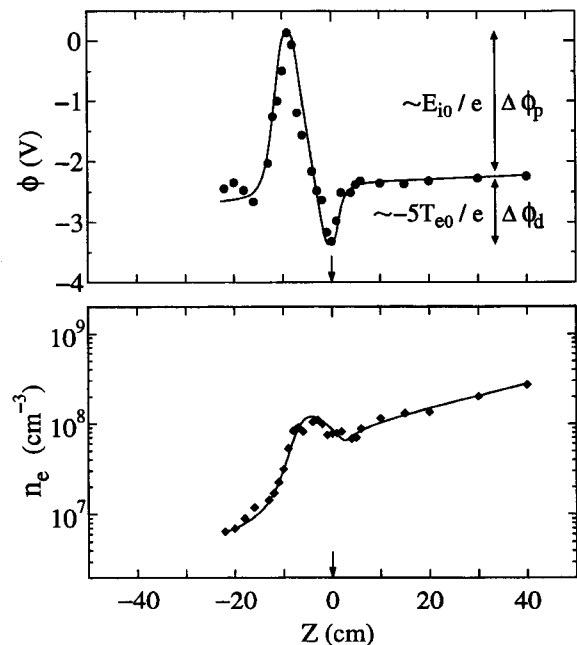


Fig. 2 Spatial profiles of plasma potential  $\phi$  and electron density  $n_e$  at  $t = 0.6 \text{ msec}$  with  $R_m = 1.68$  for  $P_\mu = 0.5 \text{ W}$ .

region due to an ambipolar diffusion. However, a stagnation of electrons is generated in the ECR region and the steep density drop is subsequently formed. Namely, the plasma flow is observed to be drastically plugged by the potential structure formed by the ECR. The electron temperature  $T_e$  increases up to  $T_e/T_{e0} = 25 \sim 30$  around the ECR region, and the  $T_e$  difference between the upstream and downstream regions is maintained.  $\Delta\phi_p$  is of the order of the ion flow energy and large enough to plug ions, so called, "plug potential".  $-\Delta\phi_d$  is about five times  $T_{e0}$ , preventing cold electrons supplied by the plasma source from merging with hot electrons in the ECR region, so called, "thermal barrier potential". Such values of  $\Delta\phi_p$  and  $\Delta\phi_d$  are plotted as functions of  $P_\mu$  with  $R_m$  kept constant as given in Fig. 3, and instead  $R_m$  with  $P_\mu$  kept constant [see Fig. 4(b): cross marks]. In any case, both  $\Delta\phi_p$  and  $-\Delta\phi_d$  increase at first, gradually saturating for larger  $P_\mu$  or  $R_m$ . It is to be remarked that the saturation value of  $\Delta\phi_p$  is always of the order of the ion flow energy  $E_{i0}$ , plugging most of the ions so as not to pass through the magnetic well region. This is because the electrons are well trapped and  $-\Delta\phi_d$  is large enough for most of the electrons to be reflected for large  $P_\mu$  or  $R_m$  under the charge neutrality condition.

Let us present results in the second case of a single-point resonance in asymmetric magnetic-well configurations. The aim of this experiment is to clarify which mirror ratio between upstream ( $R_u$ ) and downstream ( $R_d$ ) ones is more effective in the plug/barrier potential formation due to local ECR. Firstly, we change  $R_d$  with  $R_u$  kept constant 1.30 as shown in Fig. 4(a), where  $R_d$  and  $R_u$  are defined as ratios of  $B$  around  $z = -70$  cm and  $z = 100$  cm, respectively, to that at  $z = 0$  cm. The values of the plug and barrier potentials increase with an increase in the downstream mirror ratio, saturating for larger  $R_d$  for  $P_\mu = 0.8$  W, as seen in Fig. 4(b). Next, we change the upstream mirror ratio with  $R_d$  kept constant 1.68. In this case, however, no changes of the plug and barrier potentials are observed for any  $R_u$  larger than unity. Thus, the downstream mirror ratio is predominant in the plug/barrier potential formation, and only the downstream mirror ratio is needed to be increased for the confinement performance.

The third experiment is concerned with two-points resonances in symmetric magnetic-well configurations. When we decrease an average magnetic-field strength of the symmetric configuration (a), instead of the single ECR point, two ECR points appear in (b) and (c) configurations as shown in Fig. 5. In accordance with

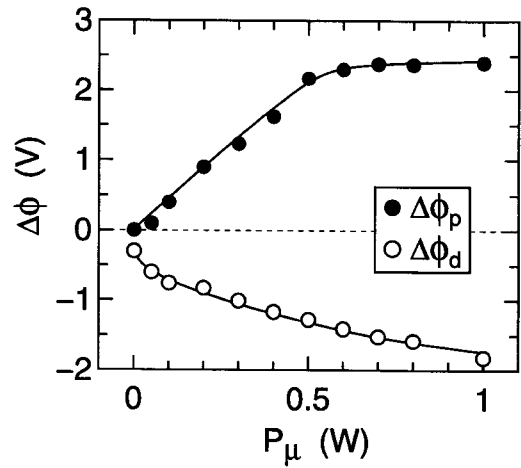


Fig. 3 Potential dip  $\Delta\phi_d$  and hump  $\Delta\phi_p$  vs  $P_\mu$  at  $t = 0.6$  msec with  $R_m = 1.68$ .

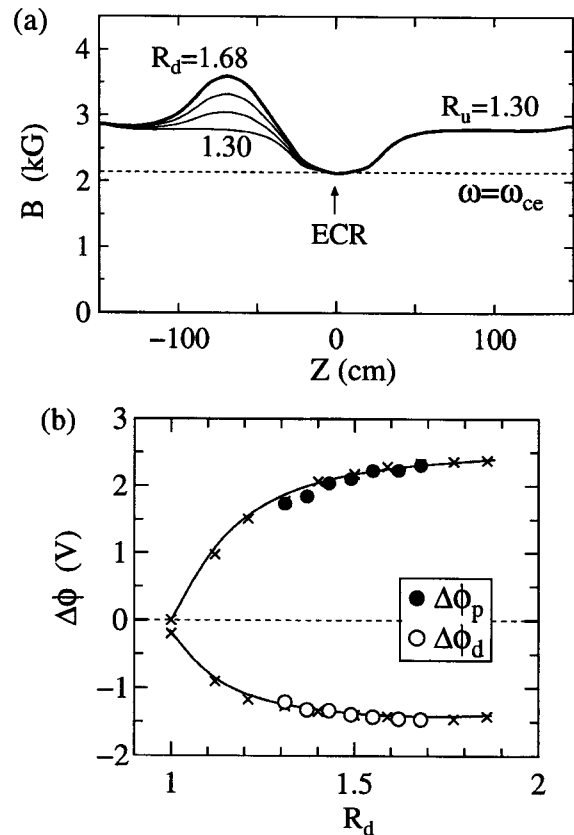


Fig. 4 (a) Asymmetric magnetic-well configuration. (b) Potential dip  $\Delta\phi_d$  and hump  $\Delta\phi_p$  vs  $R_d$  at  $t = 0.6$  msec for  $P_\mu = 0.8$  W. Crosses denote results with  $R_u = R_d$ .

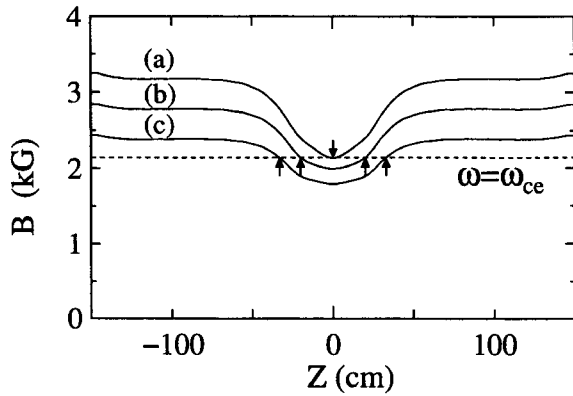


Fig. 5 Symmetric magnetic-well configuration with two-points resonances.

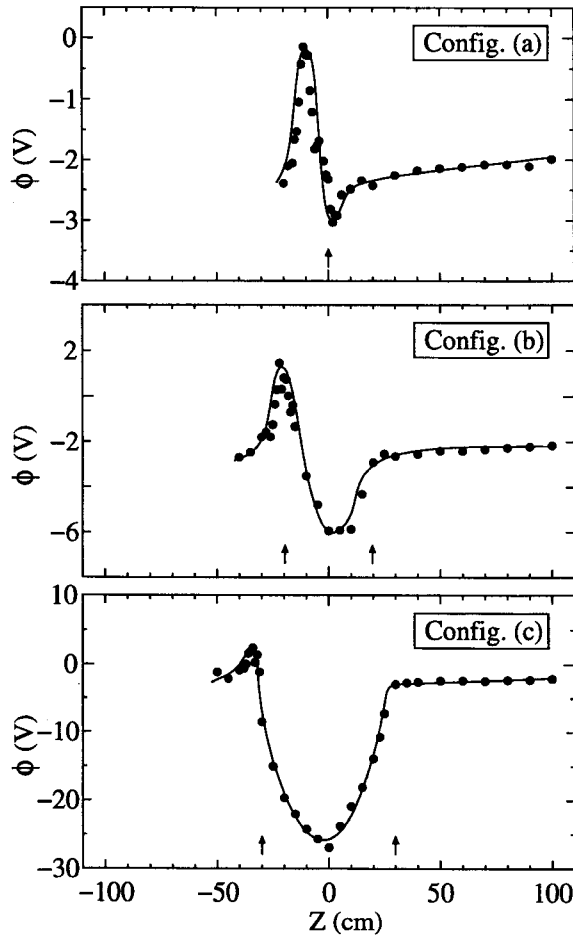


Fig. 6 Potential profiles in the magnetic configurations of Fig. 5 at  $t = 0.6$  msec for  $P_\mu = 0.5$  W.

the configuration variation, the measured potential greatly varies in profile as demonstrated in Fig. 6. Although not so appreciable change is noticed in the plug-potential value, a very deep and widespread potential well is formed as an interval of the ECR points becomes longer. Pay attention to the ordinate-scale difference (one order of magnitude difference) between (a) and (c) configurations in Fig. 6. In the configuration (c) the plug and barrier potential values are measured with the microwave power ( $P_\mu = 0 - 1$  W) as a parameter. The barrier potential depth greatly increases without saturating, being different from the plug potential height. The same tendency is obtained when  $R_m$  is increased with  $P_\mu$  kept constant in the presence of two-points resonances.

Such a strongly-modified potential profile in the barrier region is explained by an additional experimental-result in diverging magnetic-field configurations [11]. When ECR takes place at a position in a diverging-B-gradient region, the electron magnetic moment  $\mu_e (= mv_\perp^2/2B)$  increases, being accompanied by  $-\mu_e \nabla_{\parallel} B$  acceleration of electrons. Then the strong ion-acceleration potential is formed so as to maintain the charge neutrality condition.

In case of closing this section, it is to be emphasized that the potential-formation mechanism is based only on the selective electron trapping due to perpendicular  $T_e$  heating in the magnetic well and electrostatic ion trapping resulted self-consistently to satisfy the charge-neutrality condition. Such a formation of the potential structure with a positive potential region and a local minimum is the same phenomenon as a double layer formation due to the reflection of electrons in a current-carrying plasma [12,13]. Then the conventional scenario for the tandem mirror devices is not necessary, which needs two ECR points: the one for barrier formation and the other for plug formation. A single ECR is sufficient to provide the plug/barrier potential structure.

#### 4. Comparison with GAMMA 10 Results

Here we compare our basic results with results of the GAMMA 10 experiments, where only the fundamental ECRH is applied to the B-gradient region of the plug/barrier mirror cell. The representative parameters are as follows.  $\Delta\phi_p = 0 \sim 2.5$  V for  $Q_T$ -U,  $0 \sim 1.3$  kV ( $0 \sim 0.6$  kV) for GAMMA 10.  $n_e = 1 \times 10^9$  cm<sup>-3</sup> for  $Q_T$ -U and  $5 \times 10^{11}$  cm<sup>-3</sup> ( $5 \times 10^{11}$  cm<sup>-3</sup>) in the plug region for GAMMA 10.  $E_{i0} \approx 2$  eV for  $Q_T$ -U and the ion temperature parallel to the magnetic field  $T_{i\parallel} \approx 300$

eV (350 eV) for GAMMA 10. The upstream-region electron temperature  $T_{ec} = 0.35$  eV for  $Q_T$ -U and central-cell electron temperature  $T_{ec} = 60 \sim 80$  eV ( $60 \sim 80$  eV) for GAMMA 10. In the GAMMA 10 case both the two operation modes, i.e., ECRH startup [14,15] and hot ion [10], are referred, and the values written in the parentheses described just above are obtained from the experiment of the hot ion mode.

In order to be in line with the GAMMA 10 situation, on the other hand, our magnetic configuration is determined as shown in Fig. 7(a), where the ECR point is located in a  $B$ -gradient region. As expected, almost the same potential profile as described so far is experimentally confirmed. It is to be noted that there is a difference of ion velocity distribution functions between the  $Q_T$ -U and GAMMA 10 plasmas: a truncated half-Maxwellian for  $Q_T$ -U and a Maxwellian for GAMMA 10. Figure 7(b) gives the summarized result, where the plug(ECR)-region  $T_e$  at the abscissa is normalized by  $T_{ec}$ , and  $\Delta\phi_p$  at the ordinate is normalized by  $E_{i0}$  in the

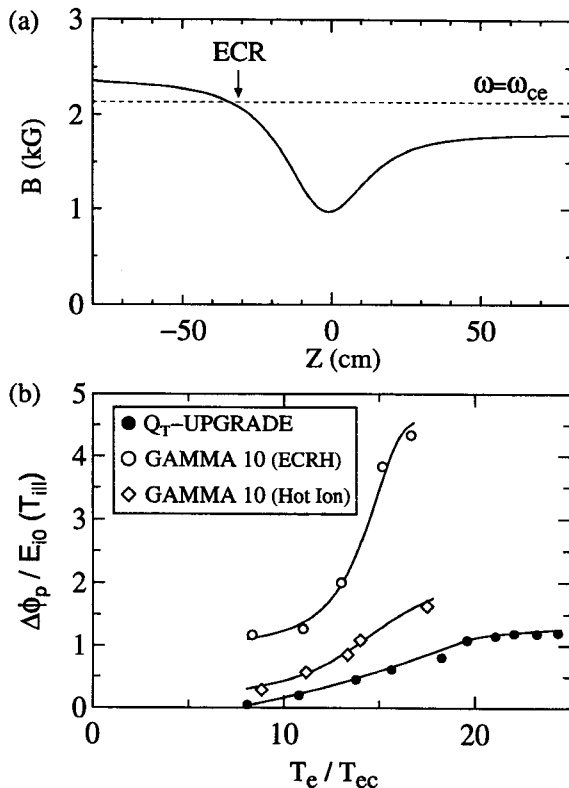


Fig. 7 (a) Magnetic configuration corresponding to the GAMMA 10 situation. (b) Comparison of normalized potential hump  $\Delta\phi_p$  vs normalized electron temperature  $T_e$  in the ECR region.

$Q_T$ -U case and  $T_{i\parallel}$  in the GAMMA case. Although the normalized  $\Delta\phi_p$  increases with an increase in the normalized  $T_e$  and appears to saturate for larger  $T_e/T_{ec}$  in a similar way in both devices, the normalized  $\Delta\phi_p$  in the GAMMA 10 attains to a value between two and four times as much as that in the  $Q_T$ -U. This is due to the difference between the ion velocity distributions and the large  $\Delta\phi_p$  is expected to plug the tail-component ions in the GAMMA 10, the detail of which is discussed later.

When the normalized  $\Delta\phi_p$  is plotted as a function of  $P_\mu$  normalized by  $n_e S$  ( $S$ : plasma cross section), the normalized  $P_\mu$  in the  $Q_T$ -U, which is required to make  $\Delta\phi_p$  large enough to plug most of the ions, is smaller than that in the GAMMA 10. This may be caused by the higher heating efficiency of the ECR in the collisionless plasma of  $Q_T$ -U while a part of the microwave power is used for a plasma production in the GAMMA 10. It is to be remarked that  $\Delta\phi_p$  in our work plays the same role on ion confinement parallel to the magnetic field as in the GAMMA 10, although  $\Delta\phi_p$  and  $E_{i0}$  in the  $Q_T$ -U are much smaller than  $\Delta\phi_p$  and  $T_{i\parallel}$  in such a big fusion-oriented device as the GAMMA 10.

## 5. PIC Computer Simulation

In order to understand physical details of the potential formation such as a  $\Delta\phi_p$  difference between  $Q_T$ -U and GAMMA 10 experiments, a PIC computer simulation with a two-and-a-half dimensional electrostatic code is performed based on a Q-machine emitter model [16]. There is a reservoir of the plasma particles at  $z = 0$  and  $x = 0.3L_x \sim 0.7L_x$ , from which electrons and ions are emitted toward a floating collector at  $z = L_z$  and  $x = 0 \sim L_x$ . An externally applied electromagnetic wave with right-hand circular polarization propagates along  $-z$  toward the reservoir, coming across a resonance point on the way. Typical simulation parameters are as follows. The charge to mass ratio:  $-1.0$  (electron),  $0.0025$  (ion). The system length:  $L_z = 512\lambda_{DeS}$ ,  $L_x = 128\lambda_{DeS}$  ( $\lambda_{DeS}$ : Debye length). The step length:  $\omega_{peS}\Delta t = 0.02$  ( $\omega_{peS}$ : electron plasma frequency). The wave electric-field strength:  $E/(T_{ec}/e\lambda_{DeS}) = 0.2$ . The subscript S stands for the parameters at the reservoir.

Figure 8 presents a typical result on the potential, electron- and ion-density profiles at  $\omega_{peS}t = 2400$  under the symmetric magnetic-well configuration of  $R_m = 2$  with the single-point resonance at  $z/\lambda_{DeS} = 256$  such as in Fig. 1. The simulation convincingly confirms the experimental result on the plug ( $\Delta\phi_p$ )/barrier ( $\Delta\phi_b$ )

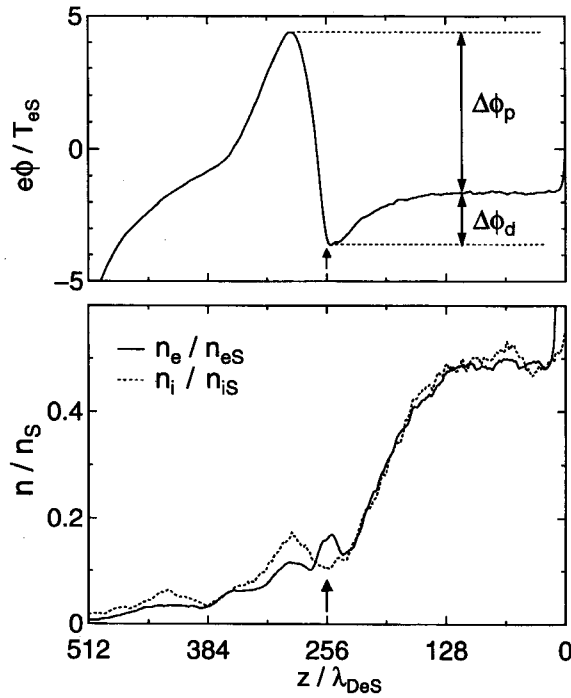


Fig. 8 Profiles of potential  $\phi$ , electron  $n_e$  and ion  $n_i$  densities in the PIC simulation at  $\omega_{eps}t = 2400$  with  $R_m = 2.0$  (single ECR point) for  $E/(T_{es}/e\lambda_{DeS}) = 0.2$ .

potential formation. In addition, the simulation for the first time clarifies a spatial deviation of the electron- and ion-density profiles, generating a charge separation to form the plug/barrier potential. This is because electrons are trapped at the  $B$ -well bottom and ions stagnate due to the potential deceleration. The separation distance  $\Delta z$  ( $\approx 40\lambda_{DeS}$ ) almost corresponds to the estimated deviation of the ion plasma oscillation around the trapped electrons, i.e., the ion Debye length ( $\approx 21\lambda_{DeS}$ ).

In order to investigate effects of the ion energy distribution function on the potential formation, the distribution ahead of the reservoir exit is systematically changed. When the ion-flow energy is increased with the ion temperature kept almost constant and on the contrary the latter is increased with the former kept almost constant, the plug potential is correspondingly increased and found to be always formed so as to reflect even the high-energy tail component in the ion distribution. This result consistently explains the  $\Delta\phi_p$ -difference between the  $Q_T$ -U and GAMMA 10.

## 6. Conclusions

According to the basic experiments on the potential formation and control due to local electron cyclotron

resonance, the following conclusions are obtained.

The plug/barrier potential is well formed and controlled with a single ECR point in mirror-type configurations of magnetic field. The scale length of the potential structure is of the order of the ion Debye length around the ECR point. The barrier potential formation is enhanced by electron trapping and/or ion acceleration due to  $\mu\nabla B$ . The plug potential is determined by the ion kinetics (self consistently formed so as to reflect ions including a higher-tail component in the velocity distribution function). The GAMMA 10 results are consistent with our simple scenario supported by the basic experiments (quantitative agreement to some extent).

## Acknowledgements

We thank M. Inutake and many scientists in the GAMMA 10 group for their useful discussion and comments. The authors are indebted to S. Ishiguro for his cooperation and H. Ishida for his assistance.

## References

- [1] T. Ohkawa, *J. Plasma Fusion Res.* **64**, 305 (1990).
- [2] D.E. Baldwin and B.G. Logan, *Phys. Rev. Lett.* **43**, 1318 (1979).
- [3] D.P. Grubb *et al.*, *Phys. Rev. Lett.* **53**, 783 (1984).
- [4] M. Inutake *et al.*, *Phys. Rev. Lett.* **55**, 939 (1985).
- [5] N. Sato, *Proc. (Invited Papers) Symp. Plasma Double Layers, Roskilde, 1982* (Risø National Laboratory, Roskilde, 1982) p.116.
- [6] J.S. Levine and F.W. Crawford, *J. Plasma Physics* **24**, 359 (1980).
- [7] T. Sato and H. Okuda, *Phys. Rev. Lett.* **44**, 740 (1980).
- [8] T. Kaneko *et al.*, *Phys. Rev. Lett.* **80**, 2602 (1998) and *J. Phys. Soc. Jpn.* **69**, 2060 (2000).
- [9] T. Tamano, *Phys. Plasmas* **2**, 2321 (1995).
- [10] K. Yatsu *et al.*, *Nucl. Fusion* **39**, 1707 (1999).
- [11] T. Kaneko *et al.*, *IEEE Trans. Plasma Sci.* **28**, 1747 (2000).
- [12] S. Torvén *et al.*, *Plasma Phys. Control. Fusion* **27**, 143 (1985).
- [13] A. Hasegawa and T. Sato, *Phys. Fluids* **25**, 632 (1982).
- [14] T. Saito *et al.*, *Proc. Int. Conf. Open Plasma Confinement Systems for Fusion, Nobosibirsk, 1993* (World Scientific, Singapore, 1993) p.121.
- [15] I. Katanuma *et al.*, *Phys. Plasmas* **3**, 2218 (1996).
- [16] S. Ishiguro *et al.*, *Phys. Plasmas* **2**, 3271 (1995).